Proceedings of the 6th International Conference on the Application of Physical Modelling in Coastal and Port Engineering and Science (Coastlab16)

Ottawa, Canada, May 10-13, 2016

TRANSPORT OF NEARSHORE DREDGE MATERIAL BERMS

DUNCAN B. BRYANT[1], BRIAN C. MCFALL[2]

1 Coastal and Hydraulics Laboratory, ERDC, USA, Duncan.Bryant@usace.army.mil

2 Coastal and Hydraulics Laboratory, ERDC, Brian.C.McFall@usace.army.mil

ABSTRACT

The transport and fate of nearshore berms are important to understand for coastal engineering applications. A physical model study was conducted in the Large-scale Sediment Transport Facility to study the transport of material placed at three cross-shore locations. In addition to measuring the hydrodynamics, surveys were conducted to measure the berm morphology. The model showed the greatest onshore migration for the berm placed nearest the shoreline, with the most offshore berm showing little on-shore or off-shore evolution. All of the berms moved asymptotically towards a stable position where the slope of the berm relief matched the slope of the facilities concrete slope (1:30). The rate of onshore transport for the shoreward berm was greater than three times that of the offshore berms.

KEYWORDS: BERMS, SEDIMENT TRANPORT, LONGSHORE TRANSPORT

1 INTRODUCTION

Dredged sediment is a resource useful in nourishing beaches, improving coastal resiliency, and maintaining and growing wetlands. Often this material can be placed as a berm in the nearshore environment to reduce the energy expended on a coastline (Zwamborn et al., 1970) and to add material to the existing profile (Vera-Cruz, 1972 and Smith et al., 2014). Currently there is little field data on the transport of these active berms under nearshore forcing. The lack of data stems from the inability to track sediment in placement projects as it mixes with native sediment. Additionally, many berm or mound placement projects have lacked comprehensive hydrodynamic forcing measurements. The combination of these two limitations in field measurements has led to limitations on predictive tools for engineering purposes.

The complex geometry of berms and limitations in nearshore coastal hydrodynamics and sediment transport modeling also complicate designing and planning of berm projects. Nearshore environments have both cross-shore and longshore flows, complex wave transformation, breaking and dissipation, turbulence generation, and complex sediment dynamics. This study uses a physical model of nearshore berms to explore the fate of dredged material placed at different depths, determine which physical processes are important, and provide data to support numerical modeling efforts.

2 PHYSICAL MODEL

A physical model study was conducted in the Coastal and Hydraulic Laboratory's Large-scale Sediment Transport Facility (LSTF) on the transport of active sediment berms in nearshore environments. The LSTF is a 30 m by 50 m basin designed to model nearshore hydrodynamics. The facility, shown in Figure 1, includes a 1 to 30 sloped concrete beach, wave generators, a longshore current recirculation system, sediment traps and instrumentation bridge. The wave generators are positioned 10 degrees from shore normal and are programmed to produce a Texel, Marsen, and ARSLOE (Atlantic Remote Sensing Land-Ocean Experiment) wave spectrum with peak periods ranging from 1.5 to 3.5s. Twenty variable speed pumps are used to match the longshore current produced by the waves allowing the facility to create a semi-infinite beach. Ten capacitance wave gauges, six Nortek Vectrino Acoustic Doppler Velocimeters (ADV), and one Nortek Profiling Vectrino ADV were used to measure the hydrodynamic conditions.

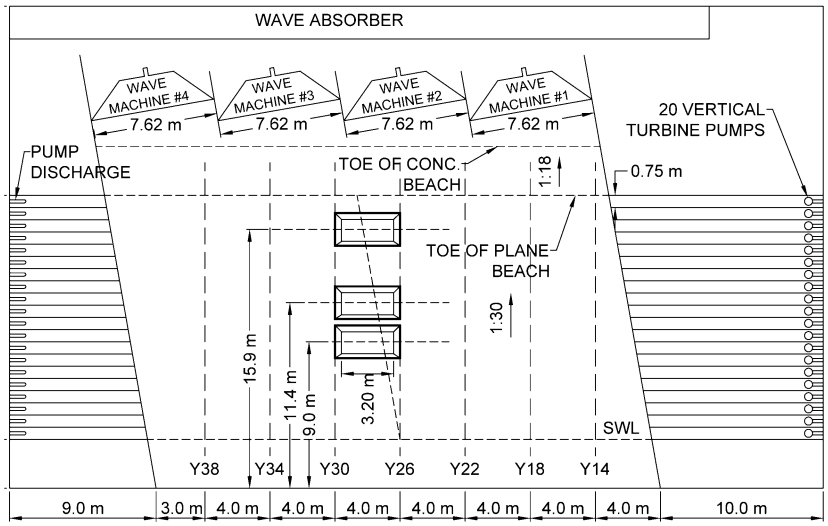

Figure 1. Large-scale Sediment Transport Facility layout with berm dimensions.

2.1 Berm Details

Berms with a volume of 1.06 m^3 were placed on the concrete beach in the nearshore at cross-shore centroid positions of 6.0, 8.4 and 12.9 m relative to the shoreline and water depths above the berm of 6, 14 and 28 cm, respectively. Well sorted fine quartz sand with a d_{50} of 0.15 mm was used to build the berms. The geometry of the berms was guaranteed by using a wooden template screed. Figure 2 is a picture of a constructed berm. The nearshore and offshore slopes are set to 28° to match the angle of final repose or angle of residual shearing (Soulsby, 1997).

Figure 2. Picture of finished berm before the instrument bridge and water level are set.

Table 1 lists the incident wave height, peak period, and cross-shore placement for the five berms presented in this paper. The berms' initial geometry was trapezoidal with a longshore length of 4m and cross-shore width of 2 m. Each berm was approximately 0.13 m in height. Profiles of the berms were conducted on regular time intervals to measure the change in berm height, shape and position. A LiDAR survey was completed after the last test to measure the berm movement and dispersal.

Table 1. Berm Test Cases

Berm	Incident H_{m0} (cm)	T_p (s)	Centroid of Berm Cross-Shore Placement (m)
B	21.4	3.5	8.42
C	16.7	1.5	8.42
E	21.4	3.5	8.42
F	16.6	1.5	6.02
G	16.7	1.5	12.92

Berm E was a repeat test of Berm B, with the same hydrodynamic conditions and berm construction. The repeat condition is used to assess the repeatability of the results due to construction and testing. Figure 3 shows the morphology of the berms from these two tests. The berms changed similarly, with a rapid reduction in height in the first 16 minutes. The change in the berm height slowed with time, and the berm moved shoreward. With an incident wave height of 21.4 cm, the berms were subjected to a large amount of longshore transport and welded to the beach as the slope of the berm relief mirrors that of the concrete floor.

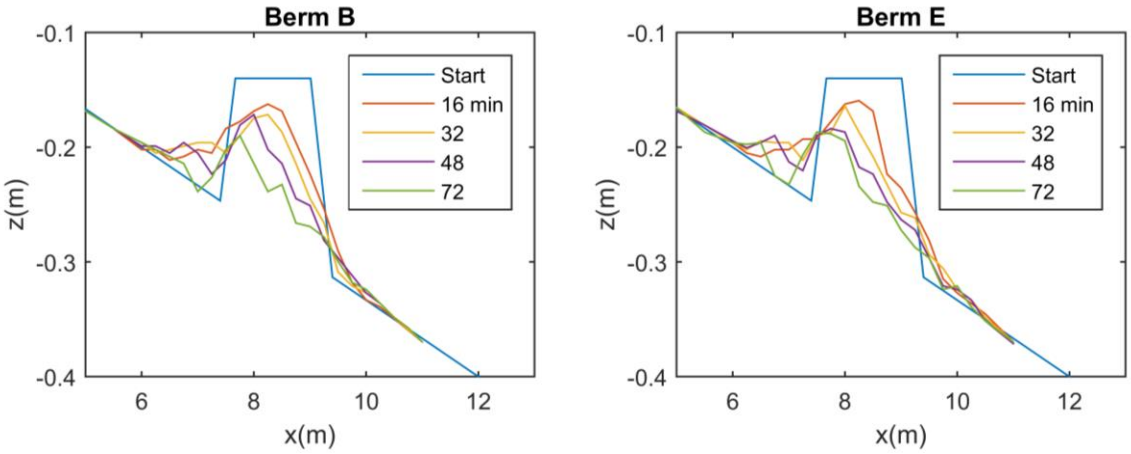

Figure 3. Evolution of identically built nearshore berms for presented forcing intervals with an incident wave height, H_{m0} = 21.4 cm and T_p = 3.5 s.

To compare the berms a number of metrics were calculated. The centroid in the cross-shore (C_x) and vertical (C_z) directions were calculated for each measured berm profile. Figure 4 shows a comparison of the centroids for Berm B and E after 16, 32, 48 and 72 minutes of testing. A line has been added to the plots to show a perfect agreement between the repeat test. Additionally the area of the berm was calculated from the centerline profiles. The centerline area is the measured berm area from a centerline survey. Berm B and E had a mean absolute difference for the cross-shore and vertical centroid of 0.08 and 0.003 m, respectively. The mean absolute difference for the berm area is 0.0054 m^2. Berm B and E show very similar morphology results giving confidence in the repeatability of the physical model.

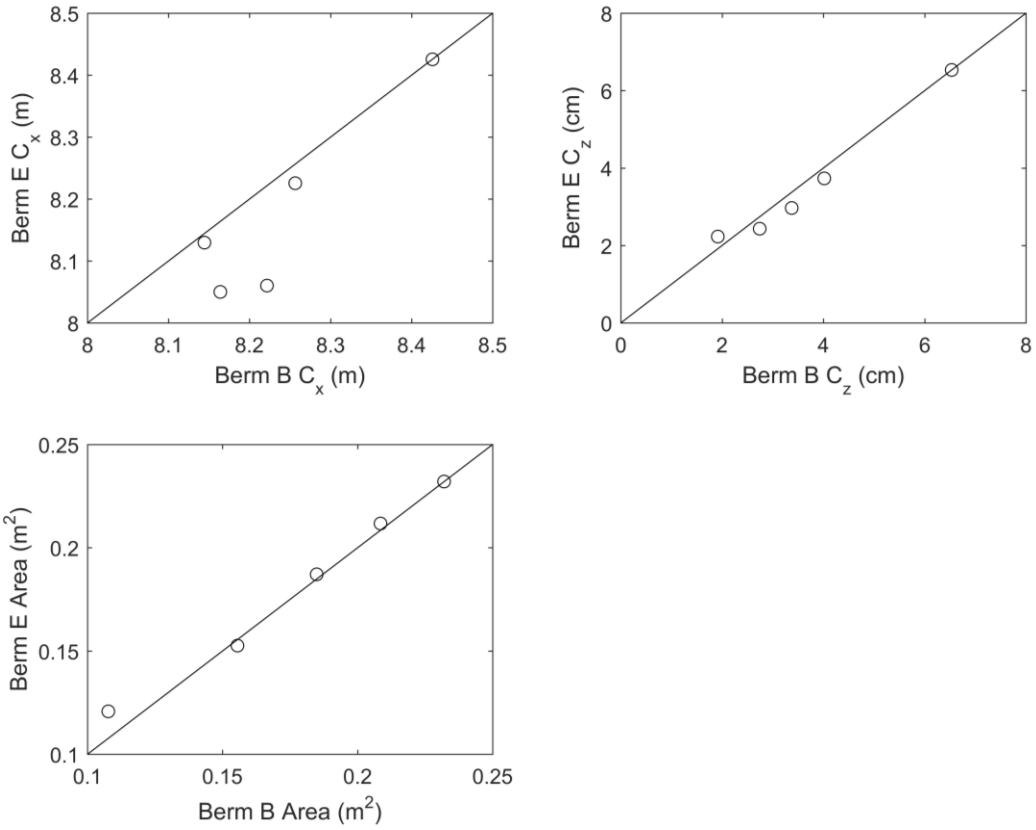

Figure 4. Comparisons for cross-shore centroid, vertical centroid and berm area of identically built nearshore berms with an incident wave height, H_{m0} = 21.4 cm and T_p = 3.5 s.

3 RESULTS

This paper focuses on the differences in berm response based on the original placement location. Berm F, C, and G all had identical forcing but varied in cross-shore location. Figure 5 shows the location of the berms on the 1:30 slope. Additionally, the figure shows the measured cross-shore significant wave height, H_{m0}, for the first 8 minutes of testing. Berm G is the most offshore of the three tested locations and due to its depth a large change in wave height over the berm is not observed. Very few waves were observed breaking over Berm G, whereas, Berm C and F had considerable wave breaking, evident by reduction in wave height over the berms (Fig. 5). This interaction of the waves with the berm considerably changed the berm morphology.

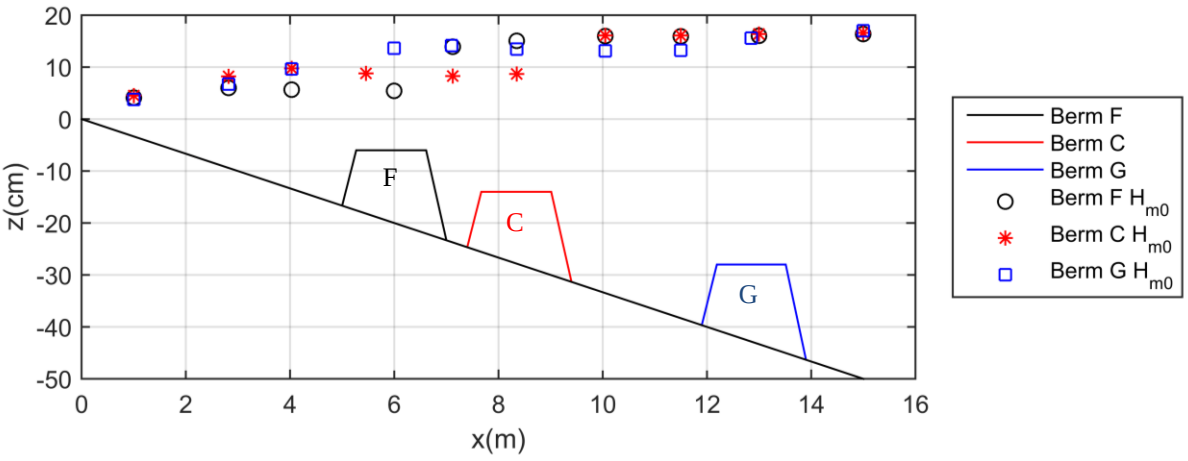

Figure 5. Measured cross-shore wave heights for the first 8 minutes of testing for Berm C, F and G.

The morphology of the berms was measured at regular time intervals and can be seen in Figure 6. Berm G, the most offshore berm, changed very little over the first 16 minutes. This berm was tested for a total of 626 minutes and like Berm B and E the relief, top of the berm, changed to a similar slope as the concrete floor. This is shown in Figure 6 as a 1:30 dashed line. Berm C is seen deflating over the course of 80 minutes and moving onshore with a relief slope similar to that of the floor. Berm F, closest to shore, moves very quickly onshore, before deflating. The time of testing is not the same for all the berms since their transport rate varied greatly.

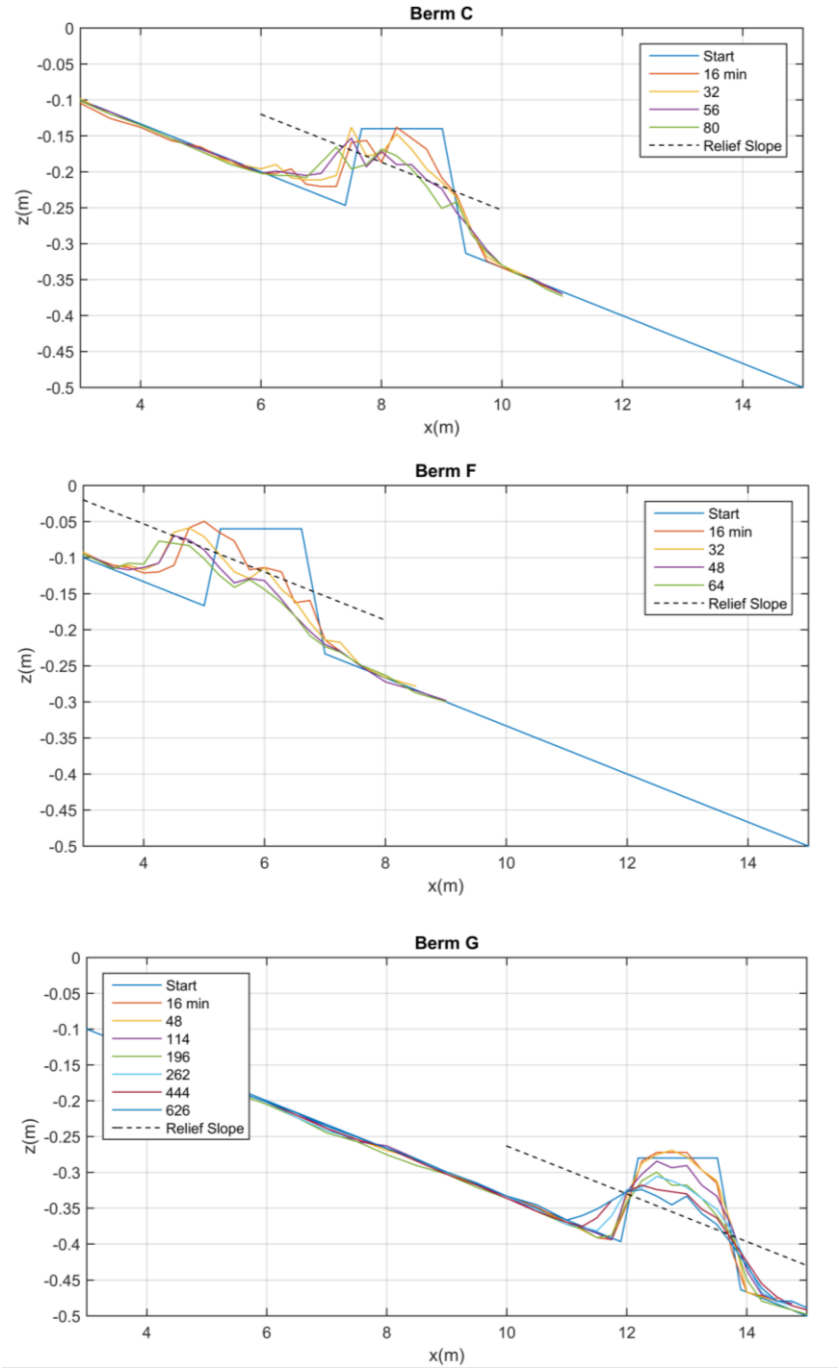

Figure 6. Measured centerline cross-shore profiles for Berm C, F, and G.

The berm cross-shore centroid, C_x, vertical centroid, C_z, and the maximum berm height above the slope, Z_{max}, were calculated to compare berm response. Figure 7 shows the change in C_x versus C_z between each profile and the beginning geometry. Additionally, Figure 7 presents the change in Z_{max} from the beginning versus time. The figure shows that all of the berms had a shoreward movement (negative C_x). Berm F located at 6.02 m initially had a maximum change in vertical centroid, Delta C_z, change of 4 cm and moved onshore 80 cm over the duration of testing. The max height also decreased by approximately 8.5 cm between the first and last profiles. The berms positioned further offshore (C and G) moved less than half of Berm F. Berm C cross-shore centroid C_x, located originally at 8.42 m offshore, moved approximately 25 cm onshore. Berm G, the most offshore berm, had centroid movement of 18 cm shoreward and 3.5 cm vertically. The transport of material shoreward in both Berm F and C is nearly linear with the reduction in berm vertical centroid equating to a proportional amount of transport shoreward. Berm G did not move onshore as quickly. Berm C and F were subjected to varying levels of breaking waves as shown by the reduction in wave height over the berm (Figure 5) acting to mobilize sediment at an increased rate. The reduction in transport for Berm G can be attributed to decreased wave velocities and lack of breaking waves in deeper water.

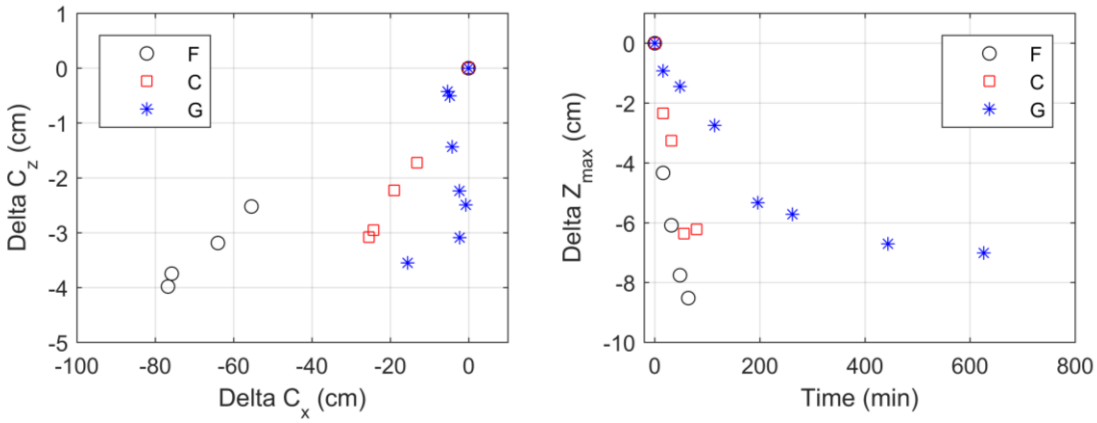

Figure 7. Change in centroids (C_z and C_x) and maximum berm height (Z_{max}) for Berm C, F, and G.

The berms are measured migrating onshore, but a portion of the berm material is lost to longshore transport. The area is calculated using the cross-shore measurements along the original berm centerline and used to infer how much material is transported in the longshore direction. Figure 8 shows the measured centerline area for berm C, F, and G. Berm F which is initially placed closest to shore has the most longshore transport, with a reduction in cross-shore area from 0.25 m^2 to approximately 0.17 m^2. Berm F experiences the greatest longshore transport because its position corresponds to the largest longshore current and it is subjected to greater sediment mobilization due to wave breaking. The further offshore berms, C and G, lose much less material to longshore transport. Interestingly, where Berm C and F appear to lose material at a constant rate with time, evident by the linear slope of the data points in Figure 8, Berm G appears to have an exponential loss of area approaching an asymptotic area. If testing on Berm C and F had been carried out further in time, this response may have been seen too.

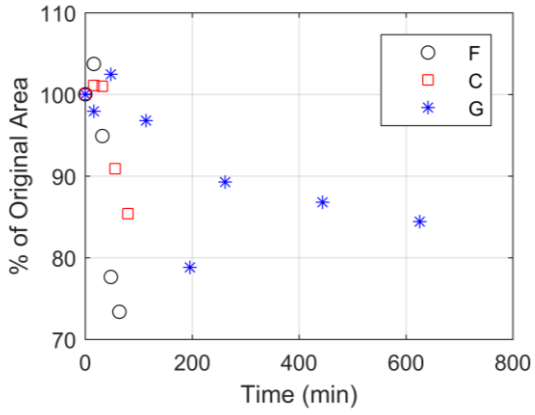

Figure 8. Change in centerline area for Berm C, F, and G.

The response time of berm migration is an important design parameter in addition to the berms final migrated position and configuration. The velocities of the centroid and Z_{max} were calculated by taking the forward difference of the centroid position and dividing by the time between measurements. Figure 9 gives the centroid and Z_{max} velocities for Berm C, F, and G. The berms show vastly different velocity in both centroid velocity and Z_{max} at the beginning of testing. Initially Berm F, the most nearshore berm and subjected to the most wave breaking, moves onshore at approximately 35 mm/min which is more than triple the initial velocity of Berm C or G. As the berm height is reduced the berm moves much slower. For all the berms presented, the centroid velocity approaches zero with time. Berm G, subjected to waves for much longer than Berm C or F, asymptotically approaches a centroid velocity of zero. When the centroid velocity reaches zero, the berm could be considered stable for the wave conditions present in the basin. More energetic waves or a change in water level would be required to further move the berm centroid. Depending on the local wave condition this may or may not happen on a favorable return period. Based on the observation with position, area, and migration velocity, the berm response may be able to be approximated with an exponential decay.

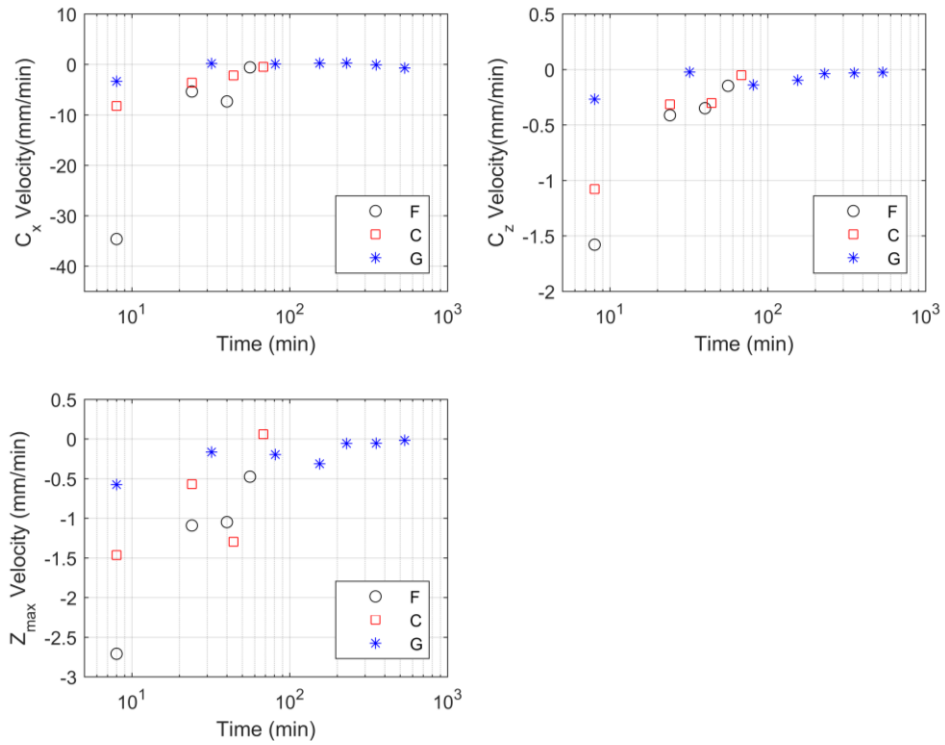

Figure 9. Centroid C_x and C_z velocity and Z_{max} velocity over testing time.

4 CONCLUSIONS

The results show that the placement depth has a considerable impact on berm migration. The most nearshore berm migrated onshore at triple the rate of the other berms, but also suffered the greatest cross-shore area loss due to longshore transport. Additionally, the most nearshore berms (F and C) reduced wave height by inducing additional wave breaking. The two berms placed further offshore had slower onshore migration and less wave height reduction. One limitation from the experiments is the response of the beach to the change in hydrodynamics resulting from a nearshore berm since the beach in this experiment is fixed and only the berm is movable. The reduced wave height shoreward of a berm may lead to additional deposition shoreward of the berm (i.e. berm acts as a submerged breakwater). In field studies this may be confused with the berm migrating further onshore, clearly presenting the need to follow the sand with physical markers or tracers. Future physical modeling efforts are planned to explore the beach profile response to the nearshore berm placement.

ACKNOWLEDGEMENT

The work is funded by the Dredging Operations and Environmental Research Program, managed by Dr. Todd Bridges, which supports the U.S. Army Corps of Engineers Navigation Operation and Maintenance Navigation Program.

REFERENCES

Smith, E. R., Permenter, R., Mohr, M. C., & Chader, S. A., 2014. *Modeling of nearshore placed dredged material.* Coastal and Hydraulics Engineering Techinical Report (Under Review). Vicksburg, MS: U.S. Army Engineer Research and Development Center.

Soulsby, R. L., 1997. *Dynamics of Marine Sands.* Thomas Telford Publications, London.

Vera-Cruz, D., 1972. Artificial nourishment of Copacabana beach. *Proc. 13th Intl. Conf. Coastal Eng.* Vancouver, Canada, 1451-1463.

Zwamborn, J. A., Fromme, G. A., & Fitzpatrick, J. B. 1970. Underwater mound for the protection of Durban's beaches. *Proc. 12th Int. Conf. Coastal Eng.* Washington D.C., USA, 975-994.